Journal of Applied Physics ARTICLE scitation.org/journal/jap

Fano resonance with high Q and figure of merit in terahertz band based on structural perturbation

Cite as: J. Appl. Phys. **132**, 233101 (2022); doi: 10.1063/5.0131487
Submitted: 21 October 2022 · Accepted: 28 November 2022 ·
Published Online: 15 December 2022

View Online Export Citation CrossMark

Guang Feng,[1] Zhihui Chen,[1,a)] Xin Liu,[1] Xiaowei Wang,[1] Xiao Liu,[1] Fei Sun,[1] Yibiao Yang,[1] Yang Wang,[2] and Shuqi Chen[3,a)]

AFFILIATIONS

[1]Key Lab of Advanced Transducers and Intelligent Control System, Ministry of Education and Shanxi Province, College of Physics and Optoelectronics, Taiyuan University of Technology, Taiyuan 030024, China
[2]Key Laboratory of Chemical Biology and Molecular Engineering of Ministry of Education, Institute of Biotechnology, Shanxi University, Taiyuan 030006, China
[3]Key Laboratory of Weak Light Nonlinear Photonics, Ministry of Education, Renewable Energy Conversion and Storage Center, School of Physics and TEDA Institute of Applied Physics, Nankai University, Tianjin 300071, China

[a)]**Authors to whom correspondence should be addressed:** huixu@126.com and schen@nankai.edu.cn

ABSTRACT

Fano resonance with high quality (Q) factor and figure of merit (FoM) has significant application prospects in biosensors and lasers. However, most of the previous studies achieve Fano resonance with high Q and FoM by directly regulating the structural asymmetry, which needs high processing precision. To maximize the Q factor of a given resonator, the best constituent material could be a hypothetical perfect electrical conductor (PEC) without ohmic losses. Here, we can indirectly regulate the asymmetry of the structure by perturbation between structures. At low asymmetry, PEC double split rings can obtain high Q factor of 374 and FoM of 257 by adjusting structural asymmetry based on structural perturbation. These are significant for Fano resonances of extremely low-loss and low ohmic losses practical application in the THz band.

Published under an exclusive license by AIP Publishing. https://doi.org/10.1063/5.0131487

I. INTRODUCTION

Terahertz (THz) spectroscopy has significant applications in many aspects due to its rich physical and chemical information characteristics. Moreover, Fano resonance can generate asymmetric sharp spectral lines and strong electromagnetic fields.[1] Therefore, the artificial photonic microstructures[2–5] at THz frequencies have significant application prospects in biosensors[6,7] and lasers.[8,9]

The performance of Fano resonance depends on its ability to capture light energy in the cavity, which is usually characterized by the Q factor. The Q factor ($Q = f_0/\Delta f$) is the ratio of the Fano resonance frequency (f_0) and the full width at half maxima (Δf).[10] However, the Fano resonance with a high Q factor has a narrow linewidth accompanied by an extremely small resonance intensity. Resonance intensity (ΔI) refers to the amplitude difference between the peak and trough of the resonant peak. To evaluate the Fano resonance, the figure of merit [figure of merit (FoM) $= Q \times \Delta I$] parameter is considered, which considers the trade-off between the Q factor and the resonance intensity.[10]

Fano resonance can be realized by single metal nanoparticles,[11] coupled plasma structures,[12,13] and dielectric structures.[14] Recently, the Fano resonance metasurfaces have been linked to the bound states in the continuum (BIC),[15–19] which is an area that has attracted more and more attention. The Fano resonance metasurfaces with broken symmetry can support high Q resonances arising from a distortion of symmetry-protected BIC. The metasurfaces in the BIC have an infinite Q factor theoretically, but they cannot couple and radiate energy outward. The quasi-BIC can achieve high Q resonances by broken symmetry. The radiative Q factor is proportional to the negative second power of asymmetry.[20] Therefore, lower asymmetry can obtain a higher Q factor. But low asymmetry needs high processing precision. Moreover, interference coupling between a multimode and a phase can achieve high Q factor.[21–23] Due to the interference between multiple modes playing an important role in the formation of high Q, the influence of multiple resonance modes on individual resonance is worth studying.

Downloaded from http://pubs.aip.org/aip/jap/article-pdf/doi/10.1063/5.0131487/16519069/233101_1_online.pdf

Published under an exclusive license by AIP Publishing

The metal and dielectric materials are widely used to achieve Fano resonance with high Q by broken symmetry. Since the plasmonic metal metasurfaces possess significant absorption, plasmonic metasurfaces cannot obtain high Q factor and FoM at low asymmetry. While at high asymmetry, the Fano resonance intensity increases but the Q factor decreases due to the increase in the radiative loss of the system. Therefore, metals can obtain relatively high FoM at high asymmetry.[10,24,25] Compared to metals, extremely low-loss dielectric materials can obtain Fano resonance with a higher Q factor. For example, $LiTiO_3$ has very high permittivity and negligible dissipation loss, which can achieve a high Q factor and FoM at low asymmetry.[26] Moreover, owing to superconducting metamaterials with extremely low radiative loss at THz frequencies, the high-temperature yttrium barium copper oxide superconductor split ring resonator has provided a higher Q factor than an identical metallic resonator at low asymmetry, which is inaccessible to high conductivity Drude metals.[25,27]

To determine the nature of Fano resonance and the ability of its enhancement, previous studies have also assumed that the ideal metal resonator is made of perfect electrical conductor (PEC) for simulation.[25,28] Therefore, periodical PEC double split rings are proposed in this work. The transmission is numerically calculated and the properties of the resonance mode are analyzed. Compared to the single split ring, double split rings can obtain higher Q factor and FoM by structural perturbation at low asymmetry. The observation of the Fano resonance behavior of PEC can provide a theoretical basis for realizing Fano resonance with high Q and FoM values for low-loss dielectrics and superconductors.

II. MODEL AND METHOD

The schematic diagram of the double split rings' resonator is shown in Fig. 1. The substrate is based on polydimethylsiloxane (PDMS), and PEC is employed for the microstructure. In this diagram, the period of the structural is P = 70 μm. The side length for the square frame is L = 60 μm. The frame width of the square frame and the gap width are D = 6 μm and G = 3 μm, respectively. The thickness of PDMS is 20 μm and the refractive index is set to a fixed value of 1.4. Meanwhile, the distance X between the upper/lower split gap and the center line of the structure is fixed at 15 μm, and the distance X1 between the middle split gap and the center line of the structure is initially 15 μm. The finite-difference time-domain (FDTD) method is used to analyze the electromagnetic properties of the structure in the simulation. The middle strip is the introduced perturbation structure.

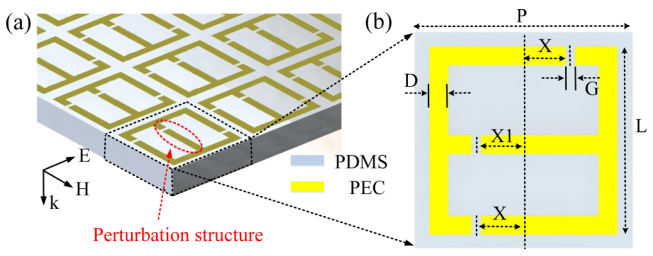

FIG. 1. (a) The double Fano resonance structure and (b) simplified two-dimensional diagram of a Fano resonance unit. The period of the structural is P = 70 μm. The side length for the square frame is L = 60 μm. The frame width of the square frame and the gap width are D = 6 μm and G = 3 μm, respectively. The distance X is fixed at 15 μm, and the distance X1 is initially 15 μm.

III. RESULTS AND DISCUSSION

Figure 2 shows the transmission obtained by simulation. The two Fano resonances with lower and higher frequencies are, respectively, denoted as FR1 and FR2. Besides, to further understand the physical mechanism of two Fano resonances, we further explain and fit the transmission by the multimode coupled oscillator model.[29] The multimode coupled oscillator model can be set as follows:

$$T = \left| \frac{2}{2 + \xi \sigma_N} \right|^2, \quad (1)$$

where $\xi = \beta(L)L/\omega\varepsilon_0\varepsilon_i$, $\beta(L)$ is the coupling constant, which is set to 0.15 here. L is the cavity length, ε_0 is the dielectric constant of the vacuum, and ε_i is the relative permittivity, which is set to 1.18 here,

$$\sigma_N = \frac{-i\omega D_1 D_2}{D_0 D_1 D_2 - D_2 K_1 - D_1 K_2}. \quad (2)$$

Here, $D_N = 1 - (\omega/\omega_N)^2 - i\gamma_N(\omega/\omega_N)(N = 0, 1, 2)$; γ_0, γ_1, and γ_2 are the attenuation coefficients of the bright mode, the first dark mode, and the second dark mode, respectively; and K_1 and K_2 are the coupling coefficients of the first dark mode and the second dark mode, respectively. The amplitude and resonance position of FR1 and FR2 can be fitted well by the multimode coupled oscillator model in Fig. 2.

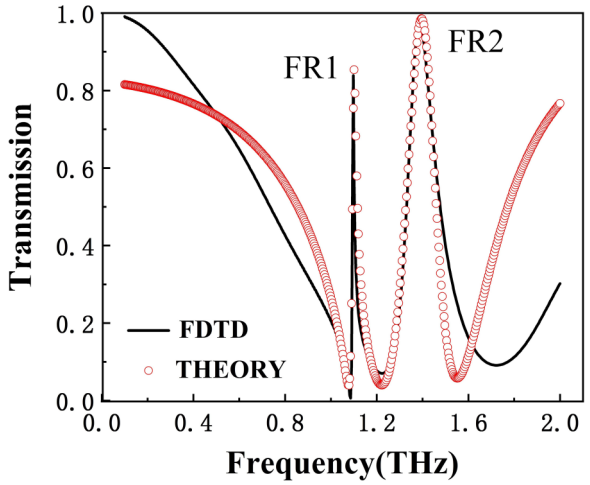

FIG. 2. Transmission of FDTD and theory. The parameters of the multimode coupled oscillator model: $\gamma_0 = 0.12$; $\gamma_1 = 0.002$; $\gamma_2 = 0.001$; $K_1 = 0.01$; and $K_2 = 0.06$.

Downloaded from http://pubs.aip.org/aip/jap/article-pdf/doi/10.1063/5.0131487/16519069/233101_1_online.pdf

Published under an exclusive license by AIP Publishing

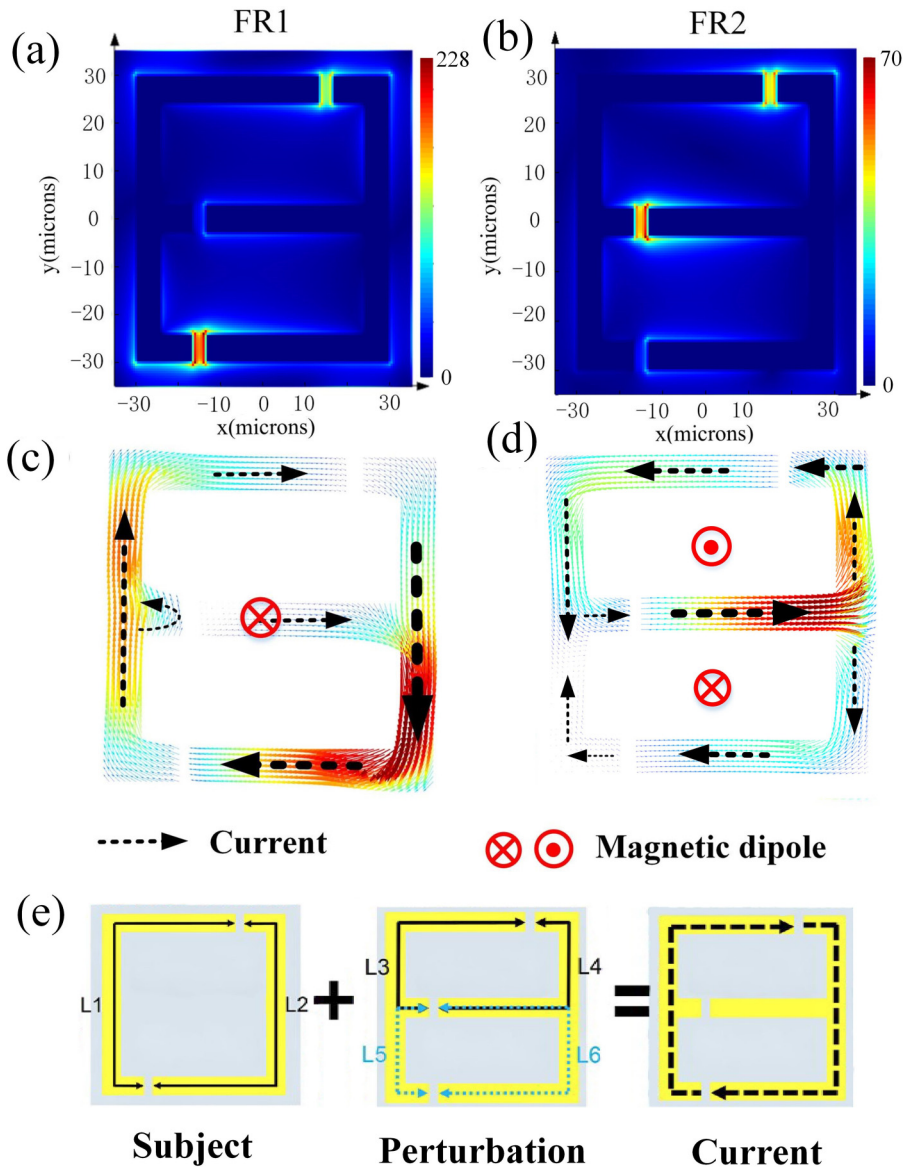

FIG. 3. (a) and (b) Electric field, (c) and (d) surface current, and (e) structural decomposition of the PEC double split rings. The black dotted arrow in (c)–(e) represents the surface current. The solid black line and the dotted blue arrow represent the length of the structure in (e).

For analyzing the origination of the two Fano resonances, the electric field and surface current of the FR1 and FR2 are shown in Fig. 3. From the electric field distribution in Fig. 3(a), it can be found that the FR1 is mainly caused by oscillation at the upper and lower split gap, while the FR2 shown in Fig. 3(b) is formed by oscillation at the middle split gap and the upper/lower split gap. Moreover, the current distributions of FR1 and FR2 are shown in Figs. 3(c) and 3(d), respectively. It can be observed from Fig. 3(c) that the excited magnetic dipole resonance associated with FR1 is attributed to the surface ring current formed in the subject structure, which refers to the outer frame of this structure, and the inner frame plays a role in perturbation. In Fig. 3(d), two magnetic dipoles can be excited, respectively, within two split rings. Due to the inverse direction of two magnetic dipoles, a toroidal dipole mode (FR2) can be formed.

Here, we mainly study FR1 with high Q factor. To analyze the cause of high Q, structural decomposition is shown in Fig. 3(e), which includes subject and perturbation parts, respectively. The subject structure plays an important role in Fano resonance, and the perturbation structure has a small effect on the surface current distribution of the subject structure. The solid black line and the dotted blue arrow represent the length of the structure in Fig. 3(e). It is obvious that the length of L1 and L2 is the same as in Fig. 3(e). According to bound states in the continuum theory,[30] the symmetrical subject structure cannot obtain Fano resonance. However, owing to the length of L3 and L4 and the length of L5

Downloaded from http://pubs.aip.org/aip/jap/article-pdf/doi/10.1063/5.0131487/16519069/233101_1_online.pdf

Published under an exclusive license by AIP Publishing

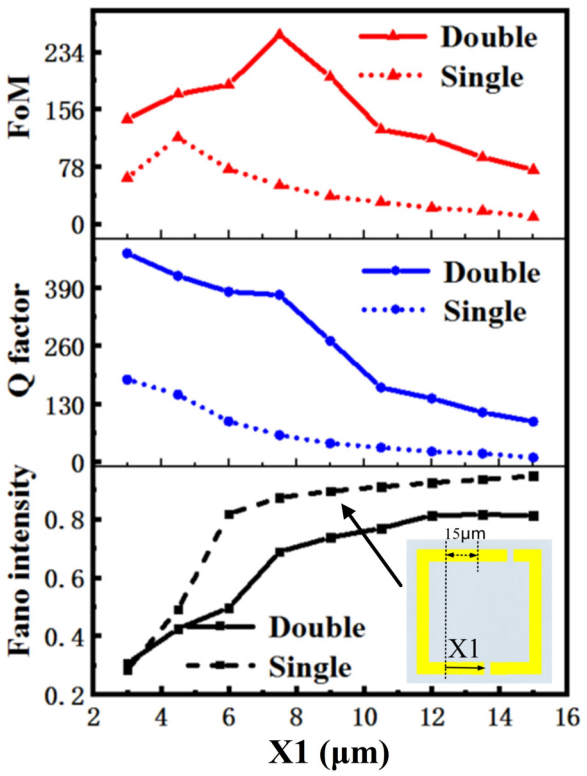

FIG. 5. The Fano intensity, Q factor, and FoM of the single and double PEC split rings with the variation of X1. The single split ring structure is shown in the illustration.

and L6 being different, the structures of L1 and L2 can form ring currents to obtain Fano resonance. Meanwhile, the difference between the asymmetry of L3 and L4 and the asymmetry of L5 and L6 is the cause of FR2.

Therefore, according to the analysis, the asymmetry of the FR1 can be empirically expressed as

$$\alpha_1 = \left|\left|\frac{L1-L2}{L1+L2}\right| - A\left|\frac{L3-L4}{L3+L4}\right| - \left|\frac{L5-L6}{L5+L6}\right|\right|. \quad (3)$$

Here, L1, L2, L3, L4, L5, and L6 are the lengths of the structure. The coupling coefficient is A. It can be seen from Fig. 5 that the Fano intensity, Q factor, and FoM value of single split ring when X1 is 6 μm are the same as those of double split rings when X1 is 15 μm. Therefore, the structural asymmetry of single and double split rings can be regarded as the same. When X1 is 6 μm, the asymmetry of the single split ring is $\alpha = |(L1-L2)/(L1+L2)| = 0.0571$, so A = 0.1485. According to formula (3), when the asymmetry of the subject structure is zero, it can obtain a very low asymmetry α_1 to achieve Fano resonance with high Q and FoM by adjusting the position of the middle split gap to deviate from the center.

The transmission of the PEC double split rings obtained by FDTD and multimode coupled oscillator model theory is shown in Fig. 4. With the distance X1 of the middle split gap varying from 15 to 0 μm, the Fano intensity of FR1 is reduced to zero. When the middle split gap locates in the center, the asymmetry of the FR1 is zero. Therefore, it cannot obtain FR1. The symmetry can be broken to obtain FR1 when the middle split gap is off-center. This result has verified the correctness of formula (3). Moreover, the theory results of Fig. 4(b) are almost the same as the FDTD results of Fig. 4(a).

For further investigating the dependence of the FR1 on the middle split gap locations, the Fano intensity, Q factor, and FoM of PEC single/double split rings with the variation of X1 are shown in Fig. 5. The single split ring structure is shown in the illustration. The single split ring fixes the position of the upper split gap on 15 μm. With X1 decreasing, the Fano intensity decreases. However, the Q factor continues to increase. Moreover, when X1 is 7.5 μm, the high Q factor and highest FoM of double split rings are 374 and 257, respectively. Compared to the Q factor and FoM of the single split ring, the Q factor and FoM of the PEC double split

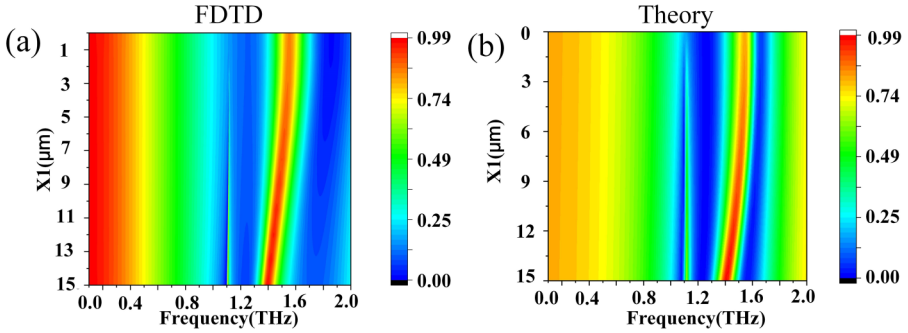

FIG. 4 The transmission of (a) FDTD and (b) theory with varying X1 from 15 to 0 μm. The parameters of the multimode coupled oscillator model: $\omega_0 = 1.38$ THz; $\omega_1 = 1.11$ THz; $\omega_2 = 1.54 - 0.00006 \times (n-50)^2$ THz; $\gamma_0 = 0.12$; $\gamma_1 = 0.002$; $\gamma_2 = 0.001 + 0.0003 \times n$; $K_1 = 0.01 - 0.0002 \times n$; and $K_2 = 0.06$. And n is 1–50 with an interval of 1.

Downloaded from http://pubs.aip.org/aip/jap/article-pdf/doi/10.1063/5.0131487/16519069/233101_1_online.pdf

Published under an exclusive license by AIP Publishing

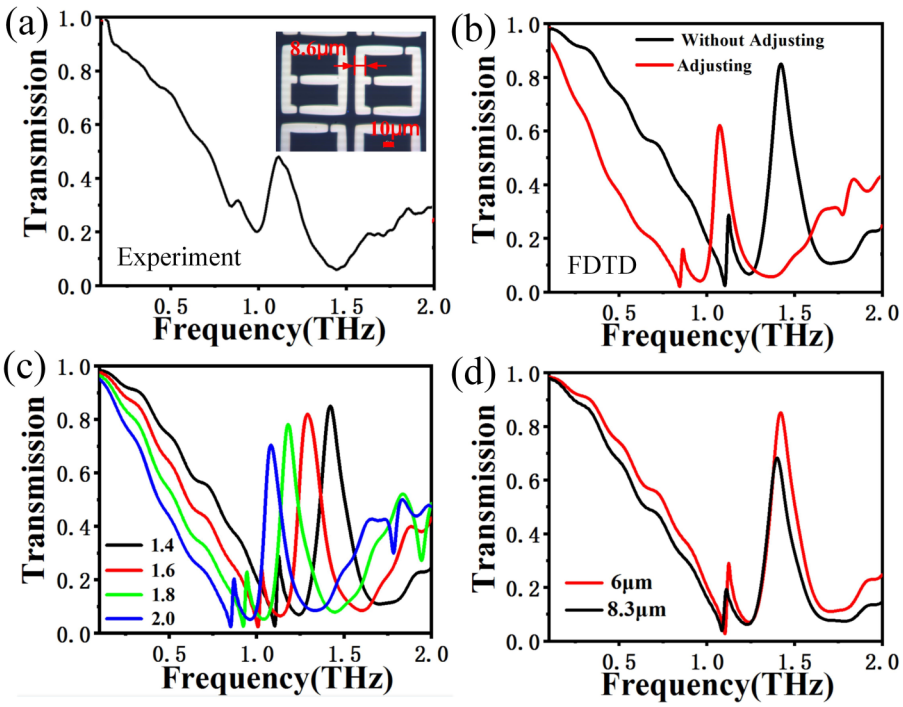

FIG. 6. (a) The experiment measured and (b) simulated transmission of Au double split rings. (c) The simulated transmission with different refractive index substrates, and (d) with a frame width of 6 and 8.6 μm. The optical image of the Au double split rings prepared in the experiment is shown in the illustration in (a). The parameters without adjusting refer to the substrate refractive index of 1.4 and the frame width of 6 μm; the parameters adjusting refer to the substrate refractive index of 2 and the frame width of 8.6 μm.

rings remarkably improve. Although PEC without ohmic losses is used here, this method provides a theoretical basis to obtain Fano resonance with high Q and FoM for low loss or even lossless dielectrics and superconductors at low asymmetry.

Moreover, to verify the transmission of double split rings, the sample of Au double split rings (2×2 cm^2) was fabricated by a standard optical lithography process. The optical image of the sample and the transmission measured by a terahertz time domain spectrometer are shown in Fig. 6(a). The resolution of the terahertz time domain spectrometer is about 3.5 GHz. Figure 6(b) shows the transmission obtained by simulation. The conductivity of Au is 4.53×10^7 S/m,[31] and the thickness of Au is 200 nm in simulation. The experimentally measured Q factor and FoM of FR1 are 17.3 and 0.9 in Fig. 6(a). While the Q factor and FoM of FR1 obtained by simulation are 26.6 and 7.0 in Fig. 6(b). There is a bit discrepancy between the measurement and simulation results. The reason for this discrepancy can be attributed to the difference between the parameters of the experiment and simulation. To analyze the discrepancy between the measurements and simulation results, the effects of the substrate refractive index and frame width on the transmission are studied by simulation in Figs. 6(c) and 6(d). Quartz glass was used in the experiment. We study the effects of substrates with different refractive indexes on transmission in Fig. 6(c). According to previous reports,[32,33] the refractive index of quartz glass is 1.9–2.1 at 0.1–2 THz. Compared to the experimental transmission in Fig. 6(a), it can be determined that the refractive index of the substrate is 2.0. The increase in the refractive index of the substrate will cause a decrease in the Fano intensity and the red shift of the Fano resonance. In addition, by observing the optical image of the sample in Fig. 6(a), the frame width of the fabricated structure is 8.6 μm. The increase in the frame width will lead to a significant decrease in the Fano intensity in Fig. 6(d). Therefore, due to the refractive index of the substrate and the frame width of double split rings in the experiment being inconsistent in the simulation, the Fano resonance in the experiment deviates from the simulation result.

Due to the limitation of experimental conditions, our experimental conditions cannot achieve the same parameters as the simulation, resulting in discrepancy in the results. However, after adjusting the parameters in the simulation according to that used in the experiment, a good consistency between the experiment in Fig. 6(a) and the simulation in Fig. 6(b) can still be obtained. Therefore, it can confirm that the numerical calculation method adopted in the simulation is correct and its results are credible. In addition, it can be found that the Fano resonances of PEC in Fig. 2 and Au in Fig. 6(b) are different. This is because the conductivity of Au is lower than that of the PEC, which suppresses the distribution of surface current. Therefore, less energy is radiated into the free space, resulting in lower Fano intensity.

IV. CONCLUSIONS

Because Fano resonance is sensitive to the symmetry of the structure, the perturbation structure can accurately adjust the asymmetry of the structure to obtain optimal Fano resonance. Compared to the PEC single split ring, PEC double split rings based on structure perturbation can obtain Fano resonance with high Q and FoM at low asymmetry. Meanwhile, we have analyzed

Downloaded from http://pubs.aip.org/aip/jap/article-pdf/doi/10.1063/5.0131487/16519069/233101_1_online.pdf

Published under an exclusive license by AIP Publishing

the structure by the multimode coupled oscillator model, which can well fit the simulation results. Moreover, the transmission of Au has been verified by experiment and simulation. The difference between the experiment and simulation is also analyzed. Although PEC does not exist in the real world and the effect of the metal is poor at low asymmetry owing to significant absorption, this method provides a theoretical basis for low loss or even lossless dielectric and superconductor to obtain Fano resonance with high Q and FoM at low asymmetry. Therefore, Fano resonance with high Q and FoM based on structural perturbation has important application prospects in biosensors and lasers.

ACKNOWLEDGMENTS

The authors thank Professor Han Jiaguang of Tianjin University for his help in the experiment. This work was supported by the National Natural Science Foundation of China (NNSFC) (Nos. U22A20258, 62175178, 61971300, and 61905208), the Central Guidance on Local Science and Technology Development Fund of Shanxi Province (No. YDZJSX2021A013), National Key Research and Development Program of China (No. 2021YFA1400601), Program for the Top Young Talents of Shanxi Province, and Program for the Sanjin Outstanding Talents of China.

AUTHOR DECLARATIONS

Conflict of Interest

The authors have no conflicts to disclose.

Author Contributions

Guang Feng: Conceptualization (equal); Writing – original draft (equal); Writing – review & editing (equal). **Zhihui Chen:** Conceptualization (lead); Funding acquisition (lead); Supervision (lead); Writing – review & editing (lead). **Xin Liu:** Software (equal); Writing – review & editing (equal). **Xiaowei Wang:** Investigation (equal). **Xiao Liu:** Software (supporting). **Fei Sun:** Methodology (supporting). **Yibiao Yang:** Formal analysis (supporting). **Yang Wang:** Data curation (supporting). **Shuqi Chen:** Conceptualization (supporting); Funding acquisition (supporting).

DATA AVAILABILITY

The data that supports the findings of this study are available within the article.

REFERENCES

[1]M. F. Limonov, M. V. Rybin, A. N. Poddubny, and Y. S. Kivshar, Nat. Photonics **11**, 543 (2017).
[2]Z. H. Chen, Y. Wang, Y. B. Yang, N. Qiao, Y. C. Wang, and Z. Y. Yu, Nanoscale **6**, 14708 (2014).
[3]Z. H. Chen, N. Qiao, Y. B. Yang, H. Ye, S. D. Liu, W. J. Wang, and Y. Wang, Sci. Rep. **5**, 12794 (2015).
[4]Z. H. Chen, N. Qiao, Y. Wang, L. Liang, Y. B. Yang, H. Ye, and S. D. Liu, Appl. Energ. **172**, 59 (2016).
[5]L. Zhou, J. Zhou, W. Lai, X. D. Yang, J. Meng, L. B. Su, C. J. Gu, T. Jiang, E. Y. B. Pun, L. Y. Shao, L. Petti, X. W. Sun, Z. H. Jia, Q. X. Li, J. G. Han, and P. Mormile, Nat. Commun. **11**, 1785 (2020).
[6]K. Shih, P. Pitchappa, M. Manjappa, C. P. Ho, R. Singh, and C. Lee, J. Appl. Phys. **121**, 023102 (2017).
[7]Y. N. Jiao, J. Lou, Z. F. Ma, L. Q. Cong, X. Xu, B. Zhang, D. C. Li, Y. Yu, W. Sun, Y. Yan, S. D. Hu, B. Y. Liu, L. Sun, R. Wang, R. Singh, Y. C. Fan, C. Chang, and X. H. Du, Mater. Horiz. **9**, 2984 (2022).
[8]A. Kodigala, T. Lepetit, Q. Gu, B. Bahari, Y. Fainman, and B. Kante, Nature **541**, 196 (2017).
[9]J. C. Jin, X. F. Yin, L. F. Ni, M. Solijacic, B. Zhen, and C. Peng, Nature **574**, 501 (2019).
[10]L. Q. Cong, M. Manjappa, N. N. Xu, I. AI-Naib, W. L. Zhang, and R. Singh, Adv. Opt. Mater. **3**, 1537 (2015).
[11]S. Campione, D. Ceglia, C. Guclu, M. A. Vincenti, M. Scalora, and F. Capolino, Appl. Phys. Lett. **105**, 191107 (2014).
[12]B. Luk'yanchuk, N. I. Zheludev, S. A. Maier, N. J. Halas, P. Nordlander, H. Giessen, and C. T. Chong, Nat. Mater. **9**, 707 (2010).
[13]W. X. Lim, M. Manjappa, P. Pitchappa, and R. Singh, Adv. Opt. Mater. **6**, 1800502 (2018).
[14]K. E. Chong, B. Hopkins, I. Staude, A. E. Miroshnichenko, J. Dominguez, M. Decker, D. N. Neshev, I. Brener, and Y. S. Kivshar, Small **10**, 1985 (2014).
[15]X. G. Zhao, C. X. Chen, K. Kaj, I. Hammock, Y. W. Huang, R. D. Averitt, and X. Zhang, Optica **7**, 1548 (2020).
[16]A. I. Ovcharenko, C. Blanchard, J. P. Hugonin, and C. Sauvan, Phys. Rev. B **101**, 155303 (2020).
[17]S. Han, L. Q. Cong, Y. K. Srivastava, B. Qiang, M. V. Rybin, A. Kumar, R. Jain, W. X. Lim, V. C. Achanta, S. S. Prabhu, Q. J. Wang, Y. S. Kivshar, and R. Singh, Adv. Mater. **31**, 1901921 (2019).
[18]L. Q. Zhu, S. Yuan, C. Zeng, and J. S. Xia, Adv. Opt. Mater. **8**, 1901830 (2020).
[19]R. S. Yang, J. Lou, F. L. Zhang, W. Zhu, J. Xu, T. Cai, Q. H. Fu, H. Q. Li, and Y. C. Fan, Adv. Photonics Res. **2**, 2100103 (2021).
[20]K. Koshelev, S. Lepeshov, M. K. Liu, A. Bogdanov, and Y. Kivshar, Phys. Rev. Lett. **121**, 193903 (2018).
[21]S. D. Liu, E. S. P. Leong, G. C. Li, Y. D. Hou, J. Deng, J. H. Teng, H. C. Ong, and D. Y. Lei, ACS Nano **10**, 1442 (2016).
[22]H. J. Li, C. S. Ji, Y. Z. Ren, J. G. Hu, M. Qin, and L. L. Wang, Carbon **141**, 481 (2019).
[23]H. J. Li, Y. Z. Ren, M. Qin, and L. L. Wang, J. Appl. Phys. **123**, 203102 (2018).
[24]S. E. Mun, H. Yun, C. Choi, S. J. Kim, and B. Lee, Opt. Mater. **6**, 1800545 (2018).
[25]Y. K. Srivastava and R. Singh, J. Appl. Phys. **122**, 183104 (2017).
[26]D. C. Zhang, Y. Wang, Y. Q. Zhu, Z. J. Cui, G. C. Sun, X. J. Zhang, Z. Y. Yao, X. Zhang, and K. Zhang, Opt. Commun. **520**, 128555 (2022).
[27]Y. K. Srivastava, M. Manjappa, H. N. S. Krishnamoorthy, and R. Singh, Adv. Opt. Mater. **4**, 1875 (2016).
[28]T. C. W. Tan, E. Plum, and R. Singh, Adv. Opt. Mater. **8**, 1901572 (2020).
[29]Z. Q. Chen, S. Zhang, Y. Q. Chen, Y. J. Liu, P. Li, Z. L. Wang, X. P. Zhu, K. X. Bi, and H. G. Duan, Nanoscale **12**, 9776 (2020).
[30]Y. J. Wang, C. W. Sun, H. Y. Li, Q. H. Gong, and J. J. Chen, Nanoscale **9**, 11085 (2017).
[31]C. Du, D. Zhou, H. H. Guo, Y. Q. Pang, H. Y. Shi, W. F. Liu, J. Z. Su, C. Singh, S. Trukhanov, A. Trukhanov, L. Panina, and Z. Xu, Nanoscale **12**, 9769 (2020).
[32]M. Naftaly and A. Gregory, Appl. Sci. **11**, 6733 (2021).
[33]C. L. Davies, J. B. Patel, C. Q. Xia, L. M. Herz, and M. B. Johnston, J. Infrared Millim. Terahertz Wave **39**, 1236 (2018).

Downloaded from http://pubs.aip.org/aip/jap/article-pdf/doi/10.1063/5.0131487/16519069/233101_1_online.pdf

Published under an exclusive license by AIP Publishing